

1 **Isotopic composition of nitrate and particulate organic matter in a**
2 **pristine dam-reservoir of western India: Implications for**
3 **biogeochemical processes**

4 Pratirupa Bardhan, S.W.A. Naqvi, Supriya G. Karapurkar, Damodar M. Shenoy, Siby Kurian,
5 Hema Naik.

6 CSIR-National Institute of Oceanography, Dona Paula, Goa:403004, India.

7 *Correspondence to:* P.Bardhan (pratirupabardhan@gmail.com)

8

9

10

11

12

13

14

15

16

17

18

19

20

21

22

23

24

25 **Abstract:**

26
27 Isotopic composition of nitrate ($\delta^{15}\text{N}$ and $\delta^{18}\text{O}$) and particulate organic matter (POM) ($\delta^{15}\text{N}$
28 and $\delta^{13}\text{C}$) were measured in Tillari Reservoir, located at the foothills of the Western Ghats,
29 Maharashtra, western India. The reservoir that is stratified during spring-summer and autumn
30 seasons but gets vertically mixed during the Southwest Monsoon (SWM) and winter is
31 characterized by diverse redox nitrogen transformations in space and time. The $\delta^{15}\text{N}$ and $\delta^{18}\text{O}$
32 values of nitrate were low ($\delta^{15}\text{N} = 2\text{-}10\text{‰}$, $\delta^{18}\text{O} = 5\text{-}8\text{‰}$) during normoxic conditions but
33 increased gradually (highest $\delta^{15}\text{N}=27\text{‰}$, $\delta^{18}\text{O}=29\text{‰}$) when anoxic conditions facilitated
34 denitrification in the hypolimnion during spring-early summer. Once nitrate was fully utilized
35 and sulphidic conditions set in, NH_4^+ became the dominant inorganic N species, with $\delta^{15}\text{N}$
36 ranging from 1.3 to 2.6‰. Low $\delta^{15}\text{N}$ ($\sim\text{-}5\text{‰}$) and $\delta^{13}\text{C}$ ($\text{-}37\text{‰}$ to $\text{-}32\text{‰}$) of POM co-
37 occurring with high NH_4^+ and CH_4 in sulphidic bottom waters were probably the consequence
38 of microbial chemosynthesis. Assimilation of nitrate in the epilimnion was the major
39 controlling process on the N-isotopic composition of POM ($\delta^{15}\text{N} = 2 - 6 \text{‰}$). Episodic low
40 $\delta^{15}\text{N}$ values of POM ($\text{-}2$ to 0‰) during early summer coinciding with the absence of nitrate
41 might arise from N-fixation, although further work is required to confirm the hypothesis.
42 $\delta^{13}\text{C}$ -POM in the photic zone ranged between $\text{-}29\text{‰}$ and $\text{-}27\text{‰}$ for most parts of the year.
43 The periods of mixing were characterized by uniform $\delta^{15}\text{N}\text{-NO}_3^-$ and $\delta^{18}\text{O}\text{-NO}_3^-$ at all depths.
44 Higher POM (particulate organic carbon (POC) as well as particulate organic nitrogen
45 (PON)) contents and C/N values with lower $\delta^{13}\text{C}$ -POM during the SWM point to
46 allochthonous inputs. Overall, this study, the first of its kind in the Indian subcontinent,
47 provides an insight into biogeochemistry of Indian reservoirs, using stable carbon and
48 nitrogen isotopes as a tool, where the monsoons play an important role in controlling vertical
49 mixing and dynamics of carbon and nutrients.

50

51 **1.Introduction:**

52 Nitrogen is an essential macronutrient the availability of which often limits primary
53 production in aquatic ecosystems. It is a polyvalent element that undergoes redox
54 transformation between the terminal oxidation states of +5 and -3. These transformations
55 involve isotopic fractionation to varying degrees, and so natural abundance of stable isotopes
56 (¹⁵N and ¹⁴N) in various N species provides useful insight into nitrogen cycling besides its
57 sources/sinks in the oceanic (Altabet, 1988; Sigman et al., 2005), coastal (Thunell et al.,
58 2004; Hu et al., 2015) and estuarine (Cifuentes et al, 1988; Savoye et al., 2012) water-bodies
59 and sediments. Studies have also been undertaken in freshwater systems like lakes (Pang and
60 Nriagu, 1977; Chen et al., 2014) and reservoirs (Chen and Jia, 2009; Junet et al., 2009). Some
61 of the best studied freshwater ecosystems in this regard are Lake Lugano at the Swiss-Italian
62 border, Lake Kinneret in Israel and Lake Superior in the USA.

63 In the eutrophic Lake Lugano, the highly depleted $\delta^{13}\text{C}$ and $\delta^{15}\text{N}$ of the near-bottom POM
64 established the active presence of methanotrophic bacteria during suboxic conditions
65 (Lehmann et al., 2004). Seasonal changes in nitrogen species were reflected in the isotopic
66 composition of particulate organic matter (POM) and dissolved inorganic nitrogen (DIN)
67 compounds in Lake Kinneret (Hadas et al., 2009). Various processes like nitrification,
68 denitrification and N₂-fixation were identified with the help of the N isotopes. In Lake
69 Superior, based on nitrate isotopic studies it was possible to identify the increasing inputs of
70 reduced N to the lake and its subsequent nitrification to be the cause behind a century-long
71 increase in the nitrate inventory of the lake, ruling out atmospheric deposition as the other
72 probable cause (Finlay et al., 2007).

73 There are a large number of natural freshwater lakes as well as man-made reservoirs in India.
74 In fact, India has the third-highest number of dams (around 4300) in the world, after China
75 and USA. However, these systems have not been well investigated for biogeochemical

76 cycling.. In the very first study of its kind, Narvenkar et al. (2013) sampled eight dam-
77 reservoirs spread across India and observed strong thermal stratification during summer in all
78 reservoirs. Six of these reservoirs were found to experience varying degrees of oxygen
79 depletion in the hypolimnia, ranging from hypoxia to complete anoxia, in spring-summer.
80 Anoxia has been found to greatly affect the distribution of nitrogen species in these systems.
81 In order to gain insights into biogeochemical cycling in these poorly investigated water
82 bodies, we selected the Tillari Reservoir for detailed studies. These included measurements of
83 natural abundance of nitrogen and oxygen isotopes in nitrate, and nitrogen and carbon
84 isotopes in POM. These data, first of their kind generated from any Indian freshwater body,
85 facilitate an understanding of biogeochemical processes (especially involving nitrogen) that
86 should be typical of any relatively pristine, tropical, monsoon-affected freshwater body.

87

88 **2.Methods:**

89 **2.1 Site Description:**

90 The Tillari Reservoir is situated in the Dodamarg *taluka* in the Sindhudurg district of
91 Maharashtra (15°76'N, 74°12'E, Fig. 1). Created by damming the Tillari River, the reservoir
92 has a maximum depth of ~50 m and a storage capacity of $0.45 \times 10^9 \text{ m}^3$ (Kurian et al. 2012).
93 The reservoir is located close to the foothills of the Western Ghats, with the drainage basin
94 having evergreen forests (C3 plant type) as well as grasslands (C3 or C4 plant types)
95 (Sukumar et al., 1995). The drainage basin of Tillari has low population density, and so the
96 river water is not much impacted by human activities such as municipal and industrial
97 discharges, and agriculture. This is reflected by high water quality (Shenoy et al., manuscript
98 in preparation). The region receives rainfall averaging around 3000 mm annually, almost
99 entirely between June and September. The evaporation rate in Tillari Reservoir is not known,
100 but for other Indian reservoirs the evaporative loss is reported to average around 0.2 m

101 (Subramanya, 2013) per month. Water from Tillari Reservoir is mainly used for irrigation.
102 Some watershed characteristics of the Tillari Reservoir have been listed in Supplementary
103 Table 1.

104 The Tillari Reservoir is a dimictic water body. Relatively low air temperatures and cool winds
105 descending from the Western Ghats, located immediately to the east of the reservoir, result in
106 convective mixing and well oxygenated conditions in winter. The water column gets
107 thermally stratified in spring and remains so until the strong SWM winds and supply of
108 relatively cold water homogenize the water column again. The water column gets stratified
109 after the SWM. Stratification during spring-summer leads to anoxic condition that is most
110 intense (sulphidic in most years) just before the onset of mixing in June-July. A previous
111 study (Kurian et al, 2012) showed that the occurrence of sulphidic conditions within the
112 euphotic zone supports anoxygenic photosynthesis by brown sulphur bacteria in this
113 reservoir. Methane has been found to accumulate in high concentrations below the
114 thermocline during this period; however, its emissions to the atmosphere are not very high
115 (Narvenkar et al., 2013). Direct human impacts on nutrient inventory of the reservoir are
116 relatively minor, as the basin is located amidst thick forests with low human population
117 density and minimum agricultural activities.

118 **2.2 Sampling and field measurements:**

119 Sampling was conducted at one station located at the deepest part of the reservoir. Water
120 samples from pre-fixed depths were collected with 5-litre Niskin samplers attached to nylon
121 ropes and equipped with reversing thermometers to measure temperature. Subsamples for
122 dissolved oxygen (DO) and hydrogen sulfide (H₂S) were collected carefully avoiding air
123 exchange. Subsamples for nutrients (nitrate and ammonium) were collected in clean 60-ml
124 HDPE bottles and frozen immediately. Subsamples for stable isotopic analyses were collected
125 in 5-litre acid-cleaned plastic carboys and transported to the laboratory within 3-4 hours.

126

127 **2.3 Laboratory analyses:**

128

129 Dissolved O₂ was estimated by the Winkler method (Grasshoff et al., 1983) with a precision
130 of <1 μM. NO₃⁻ and NH₄⁺ were measured using a SKALAR segmented flow analyzer
131 following standard procedures (Grasshoff et al., 1983) with a precision of <0.1 μM.
132 Dissolved H₂S concentration was determined colorimetrically (Cline, 1969).

133

134 **2.4 Isotopic analyses :**

135

136 Sampling for isotopic analyses of POM commenced in March 2010 and continued on a
137 monthly basis till 2012. From 2012 to 2015 samples were collected on a seasonal basis.
138 Samples for nitrate isotopic measurements were collected from 2011. The facility for nitrate
139 isotope analysis was created in 2014 and samples from 2014 and 2015 were analysed
140 immediately for natural abundance of N and O isotopes. Samples from 2011 and 2012 were
141 also analysed on a selective basis. Samples (upto 3l) for isotopic analyses of POM and DIN
142 (dissolved inorganic nitrogen i.e. NO₃⁻ and NH₄⁺) were filtered through precombusted (450° C
143 for 4 hours) 47mm GF/F filters (pore size = 0.7 μm). The filtrate was used for DIN isotopic
144 measurements and the filter papers were placed in petriplates and frozen immediately.

145

146 **2.4.1 Analyses of δ¹⁵N and δ¹⁸O of NO₃⁻:**

147 Samples for isotopic analysis of nitrate were preserved in two ways. While samples collected
148 in 2011 and 2012 were acidified with HCl to pH 2.5, those taken in 2014 and 2015 were
149 frozen immediately and analysed within a week. Prior to the isotopic analyses, nitrate and
150 nitrite concentrations were measured colorimetrically. Isotopic analyses of nitrogen and
151 oxygen in NO₃⁻ were carried out following the “chemical method” (McIlvin and Altabet,
152 2005) involving reduction of NO₃⁻ to NO₂⁻ by cadmium and further reduction to N₂O by

153 sodium azide in an acetic acid buffer. The resulting N_2O gas in the headspace was purged into
154 a GasBench II (Thermo Finnigan) and analysed in a Delta V isotope ratio mass spectrometer.
155 Nitrite concentration was insignificant in most of the samples; sulphamic acid was added in a
156 few samples that contained nitrite in concentrations exceeding $0.1 \mu M$. Working standards
157 were prepared in low-nutrient surface seawater (LNSW) collected from the Arabian Sea.
158 Calibration was done using international nitrate isotope standards USGS-32, USGS-34 and
159 USGS-35. For further quality assurance, an internal potassium nitrate standard (spanning the
160 range of nitrate concentration in the samples) was run with each batch of samples.
161 Magnesium oxide (MgO, Fisher; precombusted for 4 hours at $450^\circ C$) was added to each
162 sample to raise the pH close to 9 which was followed by addition of cadmium. We used
163 cadmium powder (Alfa Aesar, -325 mesh, 99.5%) instead of spongy cadmium as mentioned
164 in McIlvin and Altabet (2005). Each vial was wrapped in aluminium foil and placed on a
165 horizontal shaker at low speed for 17 hours. After the stipulated time, samples were removed
166 from the shaker, centrifuged and decanted into clean vials. The nitrite concentrations in the
167 decanted samples were measured to check the extent of reduction.

168 Sodium azide (2M solution) and 20% acetic acid were mixed in 1:1 proportion (by volume)
169 to yield the azide-acetic acid buffer (A-AA buffer) solution. In 20 ml crimp vials, samples
170 and standards were diluted with LNSW for a final concentration of 20 nmoles and a final
171 volume of 15 ml. Two international nitrite standards (N23 and N20) were added in this step to
172 check the efficiency of N_2O production by the buffer. After addition of the A-AA buffer, the
173 vials were allowed to stand for 1 hour and then the reaction was stopped by adding 0.5ml of
174 10M NaOH.

175 The “chemical” method yielded a very low blank ($\sim 0.5 \mu M$) and worked well for the low
176 concentration samples. The international standards were run before and after each batch of
177 samples, while the internal nitrate standards were run after every 5 samples. Analytical

178 precision (one standard deviation) was better than 0.3‰ for $\delta^{15}\text{N}$ and better than 0.7‰ for
179 $\delta^{18}\text{O}$. Results are expressed in δ notation ($\delta^{15}\text{N}$ and $\delta^{18}\text{O}$), as per mil (‰) deviation from
180 atmospheric nitrogen and Vienna Standard Mean Ocean Water (VSMOW), respectively.

181 **2.4.2 Analyses of $\delta^{15}\text{N}$ of NH_4^+ :**

182 Samples for measurements of $\delta^{15}\text{N}$ - NH_4^+ was collected during May 2012 from the anaerobic
183 hypolimnetic waters. The $\delta^{15}\text{N}$ of NH_4^+ was measured by the “ammonia diffusion” method
184 (Holmes et al., 1998). Briefly, 500 ml of sample was collected in duplicates to which 1.5g of
185 MgO was added to elevate the pH. The diffused NH_4^+ was trapped onto acidified glass-fiber
186 filter sealed between two porous Teflon membranes. The sample bottles were kept in an
187 incubator-shaker (20°C, 80 rpm) for two weeks for complete diffusion of NH_4^+ . After two
188 weeks, the GF filters were removed from each sample, dried in a NH_4^+ -free environment,
189 packed into tin cups and immediately analysed using CF-EA-IRMS. Results were corrected
190 for blank, percent recovery and fractionation. Analytical precision was better than 0.6‰.

191 **2.4.3 Analyses of $\delta^{13}\text{C}$ and $\delta^{15}\text{N}$ of POM and surface sediment:**

192 The analyses of $\delta^{13}\text{C}$ and $\delta^{15}\text{N}$ of POM were usually conducted within 1-2 months of
193 collection. The frozen filters were acid-fumed with 36% HCl to eliminate carbonates and air
194 dried in a clean laminar flow. Two aliquots (each of 12 mm diameter) were sub-sectioned
195 from each filter and packed into tin cups for analysis. Detailed methodology is given in Maya
196 et al. (2011). The $\delta^{13}\text{C}$ and $\delta^{15}\text{N}$ of POM along with particulate C and N contents were
197 analyzed in the same sample using a stable isotope ratio mass spectrometer (Thermo Finnigan
198 Delta V) connected to an elemental analyser (EURO3000 Eurovector). Results are expressed
199 as per mil (‰) deviation with respect to PDB (Pee Dee Belemnite) for $\delta^{13}\text{C}$ and atmospheric
200 nitrogen for $\delta^{15}\text{N}$. Analytical precision was better than $\pm 0.2\text{‰}$ as determined from repeated
201 measurements (after every 5 samples) of a working standard, ϵ -Amino-n-Caproic Acid

202 (ACA) having $\delta^{13}\text{C} = -25.3\text{‰}$ and $\delta^{15}\text{N} = 4.6\text{‰}$, and a laboratory sediment standard having
203 $\delta^{13}\text{C} = -21\text{‰}$ and $\delta^{15}\text{N} = 7.5\text{‰}$.

204 Surface sediment collected from the reservoir during the May 2012 field trip was analysed on
205 only one occasion to investigate its role as an ammonium source. The freeze-dried,
206 homogenized sample was analyzed following similar protocol.

207

208 **3.Results**

209 **3.1 Water column observations**

210 Based on the vertical temperature distribution it appears that the reservoir gets vertically
211 mixed through convective overturning in winter (December to February, with the exact
212 duration of mixing depending upon meteorological conditions prevailing in a given year). In
213 spring stratification sets in and is the most intense from April to June/July (with a surface-to-
214 bottom temperature difference of 7-8°C). The water column is again homogenized following
215 SWM induced mixing and flow of relatively cold water, followed by weaker stratification in
216 autumn/early winter. A detailed discussion on the physico-chemical parameters is provided in
217 Shenoy et al. (manuscript under preparation).

218 The epilimnion was always oxic. During the stratification periods, the DO concentrations
219 dropped rapidly within the thermocline. The water column became well-oxygenated
220 following the onset of the southwest monsoon. H_2S was detected below 20 m during the
221 period of intense stratification (Kurian et al., 2012), with the highest concentration recorded
222 being 9.88 μM . The occurrence of H_2S was accompanied by the appearance of CH_4 and NH_4^+ .
223 Upto 160 μM of CH_4 and 30 μM of NH_4^+ were observed in the anoxic bottom waters during
224 peak summer (Narvenkar et al., 2013) (Fig. 6).

225 A thorough analysis of nutrient dynamics in Tillari Reservoir is provided by Naik et al.
226 (manuscript under preparation). Here we provide a brief description of nitrate profiles during
227 the study period. Surface water nitrate concentrations were typically low throughout the year
228 ranging from below detection limit to 0.7 μM . However, the surface nitrate concentrations
229 were as high as $\sim 10 \mu\text{M}$ (Fig. 3a) during the SW Monsoon. Nitrate concentrations gradually
230 increased below the epilimnion during the period of weak stratification. However, with the
231 depletion of DO, nitrate concentrations in the hypolimnion decreased from 3.6 μM (at 20m)
232 to 0.3 μM (at 35m), indicating N-loss. Reoxygenation of hypolimnion during the SW
233 monsoon was accompanied by increase in nitrate concentrations (5-10 μM).

234 **3.2 Isotopic composition of nitrate and ammonium**

235 Large variations in the isotopic composition of nitrate and ammonium were observed in space
236 and time. Isotopic composition of nitrate in the epilimnion could not be measured on several
237 occasions due to low concentrations. However, when the measurements could be made it was
238 observed that the $\delta^{15}\text{N}$ and $\delta^{18}\text{O}$ values of epilimnetic (0-10 m) NO_3^- were high ($\delta^{15}\text{N} = 8$ -
239 25‰ , $\delta^{18}\text{O} = 24$ - 29‰) (Fig 3b) during the summer stratification presumably due to
240 autotrophic assimilation whereas relatively lower values ($\delta^{15}\text{N} = 5$ - 8‰ , $\delta^{18}\text{O} = 12$ - 15‰) were
241 observed during the monsoon mixing events. Increasing $\delta^{15}\text{N}$ and $\delta^{18}\text{O}$ of NO_3^- , coupled to
242 decreasing $[\text{NO}_3^-]$, were also observed in the suboxic hypolimnion during April and May,
243 when the water column was strongly stratified. The highest $\delta^{15}\text{N}$ values observed were 27.7‰
244 (in 2014) and 22.4‰ (in 2012) while the corresponding highest $\delta^{18}\text{O}$ values were 29.5‰ and
245 28.8‰ , respectively.

246 The water column remains weakly stratified for a large part of the year, usually from October
247 to March. A trend of increasing concentrations of isotopically light ($\delta^{15}\text{N} = 2$ - 8‰ and $\delta^{18}\text{O} =$
248 5 - 8‰) nitrate was observed in the hypolimnion along with gradually decreasing levels of

249 oxygen and ammonium implying the occurrence of nitrification. As the stratification
250 intensified, this phenomenon was restricted only to the metalimnion. After nitrate was
251 exhausted, high ammonium build up was observed in the bottom waters. In May 2012, NH_4^+
252 concentrations increased from 0.6 μM at 20m to nearly 12 μM at 40m with a corresponding
253 decrease in $\delta^{15}\text{N-NH}_4^+$ from 2.6‰ at 20m to 1.3‰ at 40m (Fig. 5a).

254 Elevated nitrate concentrations occur throughout the water column during the SW monsoon.
255 The $\delta^{15}\text{N}$ and $\delta^{18}\text{O}$ of NO_3^- showed little vertical variations at this time. However, interannual
256 variability was seen in the $\delta^{15}\text{N}$ of nitrate ($3.94 \pm 2.4\%$ in 2011, $11.38 \pm 1.6\%$ in 2014, and
257 $5.47 \pm 1.8\%$ in 2015), the cause of which will be examined. By contrast, the $\delta^{18}\text{O-NO}_3^-$ values
258 were relatively less variable ($13.01 \pm 4.8\%$ in 2011, $15.41 \pm 2.3\%$ in 2014, and $12.46 \pm 4.9\%$ in
259 2015).

260 3.3 Isotopic and elemental composition of suspended particulate organic 261 matter

262 The suspended particulate organic matter in the Tillari Reservoir showed distinct seasonal
263 and depth-wise variations in its isotopic and elemental compositions (Fig. 2). Primary
264 productivity in the epilimnion led to higher $\delta^{15}\text{N}$ (2‰ to 6‰) and $\delta^{13}\text{C}$ (-28% to -26%) in
265 POM and higher POC (35-60 μM) and PON (4-6 μM) contents as compared to the bottom
266 water. The molar C/N ratios in the surface waters ranged between 7 and 10. Depleted $\delta^{15}\text{N}$
267 ($\sim -1.4\%$) in the epilimnion was observed during the early stratification period (February and
268 March). As the stratification intensified, the $\delta^{15}\text{N}$ and $\delta^{13}\text{C}$ of the epilimnetic POM became
269 heavier, presumably reflecting a gradual enrichment of heavier isotopes in the dissolved
270 inorganic N and C pools. Both $\delta^{15}\text{N}$ and $\delta^{13}\text{C}$ decreased with depth with the lowest values
271 occurring in the anoxic bottom water during peak stratification period. The C/N values in
272 these waters were in the range of 4-7. In terms of seasonal variability, $\delta^{13}\text{C}$ values of POM

273 were lower during monsoon mixing and became more enriched as the stratification
274 intensified. The $\delta^{15}\text{N}$ values, however, did not depict any distinct seasonal pattern. High POC
275 (upto 80 μM) and PON (upto 9 μM) along with high C/N (>10) were recorded during the
276 monsoon season apparently reflecting allochthonous inputs.

277 **4. Discussion:**

278 **4.1 Epilimnetic processes:**

279 Nitrate concentrations in surface waters of the Tillari Reservoir varied from below detection
280 limit during the premonsoon period to 10.7 μM during the SW monsoon. The $\delta^{18}\text{O}$ and $\delta^{15}\text{N}$
281 values of nitrate in the epilimnion were high, a signature of assimilation: phytoplankton
282 prefer nitrate containing ^{14}N and ^{16}O leaving residual nitrate enriched with $\delta^{15}\text{N}$ and $\delta^{18}\text{O}$
283 (Casciotti et al., 2002). We examined the slopes of the $\delta^{18}\text{O}$ vs. $\delta^{15}\text{N}$ regression in the surface
284 water. While a 1:1 line would represent assimilation of epilimnetic nitrate, a steeper slope
285 would imply assimilation along with the regeneration of nitrate via nitrification (Wankel et
286 al., 2007). We observed a nearly 1:1 trend for most of the surface water samples during the
287 summer stratification implying that assimilation exerts the major control on surface NO_3^-
288 isotopic composition (Supplementary Fig. 1).

289 The isotopic composition of the DIN source exerts the key control on the $\delta^{15}\text{N}$ of POM
290 (Altabet, 2006). The epilimnetic POM in the Tillari Reservoir is expected to have $\delta^{15}\text{N}$ less
291 than or equal to the $\delta^{15}\text{N}\text{-NO}_3^-$. Indeed, the $\delta^{15}\text{N}\text{-POM}$ was always lower than the $\delta^{15}\text{N}$ of the
292 source nitrate (Fig. 3b). The range of $\delta^{13}\text{C}$ values of surface-water POM (-32 to -26‰) was
293 typical of lacustrine autochthonous organic matter (-42 to -24‰, Kendall et al., 2001 and
294 references therein). As the summer progressed, productivity increased resulting in increased
295 CO_2 uptake and elevated $\delta^{13}\text{C}\text{-POM}$. During photosynthesis, phytoplankton preferentially

296 uptake ^{12}C leaving the DIC (dissolved inorganic carbon) pool enriched in ^{13}C . However, when
297 dissolved C is scarce and/or growth rate is high, the phytoplankton would consume the
298 available DIC with reduced or no isotopic discrimination. As the summer progressed at the
299 study location, increased water temperature and low dissolved inorganic nutrient and DIC
300 concentrations would cause the phytoplankton to express reduced isotopic discrimination.
301 This would result in enriched $\delta^{13}\text{C}$ of POM. Similar enrichment of $\delta^{13}\text{C}$ -POM during periods
302 of high productivity have also been observed in other lakes, for e.g., Lake Lugano (Lehmann
303 et al., 2004) and Lake Wauberg (Gu et al., 2006).

304 In March, when nitrate was close to detection limit, surface $\delta^{15}\text{N}$ -POM was -1.4‰ . The POM
305 resulting from nitrogen fixation by cyanobacteria usually has a $\delta^{15}\text{N}$ of 0 to -2‰ (Carpenter
306 et al., 1997). Zeaxanthin, marker pigment of cyanobacteria, was present in significant
307 concentrations ($305.1 \pm 21 \text{ ng l}^{-1}$) within the epilimnion, whereas Chl-*a* concentration was ~ 1.7
308 $\mu\text{g l}^{-1}$ (S. Kurian, unpublished data). However, measurements of nitrogen fixation rates in the
309 Tillari Reservoir have yielded very low values during summer (unpublished data).
310 Alternatively, the lower $\delta^{15}\text{N}$ values may also result from isotopically light nitrate that is
311 produced in the hypolimnion and diffuses upward into surface waters. Another possible
312 source of isotopically lighter N could be atmospheric deposition, although the magnitude of
313 atmospheric inputs is not expected to be very large during early summer. Further work is
314 required to understand the episodic occurrence of low $\delta^{15}\text{N}$ -POM.

315 **4.2 Biogeochemistry of hypolimnion**

316 **4.2.1 Nitrification:**

317 Stratification in the Tillari Reservoir sets in soon after the decline of the monsoon-fed inflow
318 following which nitrate concentrations increased in oxygenated bottom waters with a
319 concomitant decrease in ammonium concentrations, indicating the occurrence of nitrification.

320 The nitrate concentrations ranged from below detection limit in the upper 10 m to nearly 10
321 μM close to the bottom. Nitrification occurs in two steps: ammonia oxidation to nitrite
322 (performed by ammonia oxidising archaea and bacteria) and nitrite oxidation to nitrate
323 (performed by nitrite oxidising bacteria). Ammonium, the primary N source, undergoes
324 strong fractionation producing isotopically light nitrate (Delwiche and Stein, 1970, Casciotti
325 et al., 2003). The $\delta^{15}\text{N}\text{-NO}_3^-$ values ranged from 2-10‰ and the $\delta^{18}\text{O}\text{-NO}_3^-$ ranged from 5-
326 8‰ during this period. Nitrate accumulation due to atmospheric deposition and microbial
327 nitrification will have distinct $\delta^{18}\text{O}\text{-NO}_3^-$ values. This is because, while the oxygen atoms in
328 atmospheric nitrate are derived from interactions between NO_x and O_3 in the atmosphere,
329 those in nitrate produced by nitrification come from dissolved oxygen and water (Kendall,
330 1998, Finlay et al., 2007). This is well reflected in the $^{15}\text{N}\text{-}^{18}\text{O}$ scatter plot where the $\delta^{18}\text{O}\text{-}$
331 NO_3^- data-points from the epilimnion and hypolimnion form completely distinct clusters in
332 February (Fig 4). As the ammonium pool gets used up, the nitrification rate decreases
333 accompanied by a decrease in the extent of fractionation (Feigin et al., 1974).

334 Ammonium, oxygen and carbon dioxide are the major substrates needed for nitrification
335 (Christofi et al., 1981). While ammonium largely comes from the sediments, oxygen is
336 supplied from aerated surface waters. During the early stratification period, conducive
337 conditions exist for nitrifiers to grow within the hypolimnion. However, as the bottom waters
338 turn increasingly more oxygen-depleted with the intensification of stratification the
339 “ammonium-oxygen chemocline” (Christofi et al., 1981) moves upward in the water column
340 and the metalimnion becomes more suitable for the occurrence of nitrification. In April 2014,
341 $\delta^{18}\text{O}$ declined within the thermocline from 34‰ at 5m to 14‰ at 20m owing to nitrification.
342 Epilimnetic nitrate isotope data are not available for 2012 due to very low nitrate
343 concentrations. However, the $\delta^{18}\text{O}$ declined from 25‰ at 15m to 17‰ at 20m. The $\delta^{15}\text{N}$
344 values in both the years did not show a similar decline, but this is consistent with the results

345 of several other studies (Böttcher et al., 1990; Burns and Kendall, 2002), where the $\delta^{18}\text{O}$ was
346 found to be better suited for source and process identification than $\delta^{15}\text{N}$. It may be noted that
347 this decoupling of $\delta^{15}\text{N}$ and $\delta^{18}\text{O}$ was only observed during the peak stratification period at
348 the thermocline.

349 The $\delta^{15}\text{N}$ and $\delta^{13}\text{C}$ values for the POM were generally low during the nitrification period as
350 also observed in Lake Kinneret (Hadas et al., 2009). The $\delta^{15}\text{N}$ varied from -4‰ to 3‰ while
351 $\delta^{13}\text{C}$ varied from -31‰ to -29‰ . Assimilation of newly nitrified NO_3^- may be a possible
352 contributor to POM as indicated by the low $\delta^{15}\text{N}$ values.

353 **4.2.2 Denitrification:**

354 During the period of strong stratification, the water column loses oxygen below the
355 thermocline, which apparently results in N loss. Along with a decrease in nitrate, there also
356 occurs an increase in NH_4^+ concentration. Dissimilatory nitrate reduction is known to be
357 associated with 1:1 increase in $\delta^{15}\text{N-NO}_3^-$ and $\delta^{18}\text{O-NO}_3^-$ (Granger et al., 2008). Linear
358 regression of $\delta^{18}\text{O}$ versus $\delta^{15}\text{N}$ yielded slope values of 0.95 and 0.85 in 2014 and 2012,
359 respectively. In canonical denitrification, both $\delta^{15}\text{N-NO}_3^-$ and $\delta^{18}\text{O-NO}_3^-$ increase linearly.
360 The enrichment in isotopic value is ~ 1 in marine systems (Casciotti et al., 2002, Sigman et
361 al., 2005, Granger et al., 2008). However, this value is reported to be lower (0.5-0.7) in
362 freshwater systems (Lehmann et al., 2003 and references therein). The reasons for this
363 difference are not fully understood. Also, studies in freshwater systems are sparse as
364 compared to marine systems. In a batch of culture experiments, Granger et al. (2008)
365 observed that nitrate-reducing enzymes play a role in altering the O to N isotopic enrichment,
366 with periplasmic dissimilatory nitrate reductase (Nap) expressing a lower enrichment value
367 (~ 0.62) than the membrane-bound dissimilatory nitrate reductase. Again, there is a lack of
368 data on the isotopic expressions of these enzymes at the ecosystem level. Wenk et al. (2014)

369 attributed the low O:N isotopic effect of ~ 0.89 to chemolithoautotrophic denitrification,
370 rather than heterotrophic denitrification, in the northern basin of Lake Lugano.

371 Our data from the Tillari reservoir indicates the occurrence of denitrification in the suboxic
372 hypolimnion under stratified conditions. However, this process is restricted to a narrow depth
373 range of 10-20 m which limits the number of data points. There may be several factors
374 responsible for the low (< 1) isotopic enrichment factor in the Tillari but our data are not
375 sufficient to identify the exact cause(s).

376 Assuming the N loss was largely through denitrification, an attempt was made to compute the
377 fractionation factor using a Rayleigh “closed-system” model (Lehmann et al., 2003).
378 Although there have been several attempts to compute the nitrogen isotope enrichment
379 factors in marine systems, ground waters and laboratory cultures (Table 1); similar
380 information is relatively scarce from freshwater lakes and reservoirs.

381 The available information on oxygen isotope fractionation is even scarcer. The values of ϵ^{15}
382 and ϵ^{18} computed by us are -8.7‰ and -10.7‰ , respectively. The ϵ^{15} is much lower than
383 those obtained from laboratory cultures (Olleros, 1983; Table 1) as well as open-ocean OMZs
384 (Brandes et al., 1998, Voss et al., 2001; Table 1) although it is close to the ϵ^{15} reported from
385 the eutrophic Lake Lugano. Factors controlling denitrification rates in aquatic systems
386 include temperature, availability of nitrate and organic carbon, oxygen concentration and type
387 of bacterium involved (Seitzinger et al., 1988, Bottcher et al., 1990, and references therein).
388 Sedimentary denitrification is known to incur isotope effect (ϵ^{15}) of $\sim 0\text{‰}$ due to almost
389 complete exhaustion of nitrate. The dissolved nitrate concentrations in the Tillari Reservoir
390 are quite low with the highest values being in the range of 10-12 μM (see Results). The
391 hypolimnetic nitrate concentrations were even lower ($< 5 \mu\text{M}$) during periods of anoxia. Low
392 nitrate availability and sedimentary N-loss may exert major controls on the low ϵ^{15} observed
393 in the Tillari Reservoir.

394 Denitrification strongly discriminates among the two N isotopes, leaving behind ^{15}N -enriched
395 in the residual NO_3^- . POM produced by assimilation of this nitrate will also be enriched in
396 ^{15}N . However, lower $\delta^{15}\text{N}$ -PON at these depths implies that NH_4^+ was the preferred DIN
397 source. For instance, observations in April 2012 showed that denitrification was active below
398 30m and associated with ammonium build-up, there was nearly a 4‰ depletion in $\delta^{15}\text{N}$ -PON
399 from 2.5‰ (at 30m) to -2.3‰ (at 40m).

400 **4.2.3 Ammonification:**

401 The isotopic composition of ammonium should reflect that of the sedimentary organic matter
402 being degraded. In Lake Kinneret (Israel), $\delta^{15}\text{N}$ - NH_4^+ values in the hypolimnion during
403 stratified conditions ranged from 12 to 17 ‰ reflecting the high $\delta^{15}\text{N}$ of the sedimentary OM
404 ($\delta^{15}\text{N} = 10\text{‰}$) (Hadas et al., 2009). In Lake Bled (NW Slovenia), mean $\delta^{15}\text{N}$ - NH_4^+ value of
405 3.8‰ was similar to that of sedimentary OM ($\delta^{15}\text{N} = 4.5\text{‰}$) (Bratkic et al., 2012). Likewise,
406 the sedimentary OM in the Tillari Reservoir had a $\delta^{15}\text{N}$ of 2.96‰ similar to the $\delta^{15}\text{N}$ - NH_4^+
407 (1.3-2.6‰) thus establishing remineralization of sedimentary OM as the principal NH_4^+
408 source.

409 A negative linear relationship between $\delta^{15}\text{N}$ -PON and $\ln[\text{NH}_4^+]$ was observed (Fig. 5b) which
410 further indicated uptake of NH_4^+ . Although this relation was mainly determined by the low
411 $[\text{NH}_4^+]$ and high $\delta^{15}\text{N}$ -PON observed at the top of the hypolimnion (20m), it is important to
412 include this datapoint to highlight the rapid decline of $\delta^{15}\text{N}$ -PON over a short depth range.
413 The fractionation factor (ϵ) calculated from the slope was -2.4‰. The fractionation factor for
414 ammonium assimilation has been estimated in several field studies (Cifuentes et al., 1988;
415 Bratkic et al 2012) as well as in lab cultures with different organisms (green algae, marine
416 bacteria, etc) (Wada & Hattori, 1978, Wada 1980, Hoch et al 1992). However, such studies in
417 freshwater lakes and reservoirs are scarce. Bratkic et al. (2012) computed fractionation

418 factors of -0.8‰ and -1.4‰ for mean ammonium concentrations of $4.7\ \mu\text{M}$ and $3.3\ \mu\text{M}$
419 respectively in Lake Bled. Hoch et al. (1992) reported fractionation factor for assimilation by
420 *Vibrio harveyi*, a marine bacterium, to be between -4‰ and -27‰ for ammonium
421 concentrations ranging from 23 to $180\ \mu\text{M}$. The fractionation factor is expected to approach
422 0‰ for decreased concentrations of ammonium. For the low to moderate ammonium
423 concentrations recorded (maximum $\sim 12\ \mu\text{M}$ in Figure 5) the fractionation factor computed by
424 us compares well with previously reported values.

425 4.2.4 Sulphate reduction and evidence for chemosynthesis:

426 As the summer intensified and oxidized nitrogen was fully utilized, facultative bacteria
427 apparently began to utilize sulphate as an electron acceptor as indicated by the accumulation
428 of H_2S . Mass dependent fractionation during microbial degradation of organic matter with
429 sulphate as an electron acceptor would the residual organic matter enriched in ^{13}C and ^{15}N .
430 However, following the appearance of H_2S , both $\delta^{13}\text{C}\text{-POC}$ and $\delta^{15}\text{N}\text{-PON}$ became more
431 depleted. The $\delta^{15}\text{N}$ values varied between -8‰ and -5‰ and $\delta^{13}\text{C}$ values ranged from -37‰
432 to -32‰ between 30 and 40m depths. The accumulation of H_2S was also accompanied by
433 significant build-up of CH_4 ($20\text{-}150\ \mu\text{M}$) and NH_4^+ ($1\text{-}20\ \mu\text{M}$) (Naik et al., manuscript in
434 prep.). Increases in POC and PON contents were also observed: from $28\ \mu\text{M}$ to $60\ \mu\text{M}$ for
435 POC and from 4.7 to $8\ \mu\text{M}$ for PON. Bacterial assimilation of ammonium can explain the
436 isotopically light nitrogen, but utilization of biogenic methane is known to lead to extremely
437 low $\delta^{13}\text{C}$ values (between -65‰ and -50‰ ; Whiticar et al., 1986). In our study, the most
438 depleted $\delta^{13}\text{C}\text{-POC}$ value of -37.8‰ was associated with the highest methane concentration
439 of $156\ \mu\text{M}$. Interestingly, in a study carried out in the waters of Lake Baikal in Siberia, very
440 negative $\delta^{13}\text{C}\text{-DIC}$ values (-28.9 to -35.6‰) were inferred to be derived from methane
441 oxidation while the $\delta^{13}\text{C}\text{-POC}$ values (-31.7 to -33.5‰) were typical of lacustrine organic

442 matter (Prokopenko and Williams 2005). The authors explained this lack of correlation
443 between the two C pools by a possible time lag between the peak methane oxidation and peak
444 productivity. Low $\delta^{13}\text{C}$ -POC ($\sim -37\text{‰}$) in Lake Kinneret was attributed to chemosynthetic C
445 fixation using depleted $\delta^{13}\text{C}$ -DIC derived from methane oxidation (Hadas et al. 2009). It is
446 important to understand the fate of methane in freshwater systems as they are believed to be
447 significant contributors to atmospheric methane emissions (Bastviken et al., 2004). The
448 POM isotopic data of the Tillari Reservoir provides evidence for intense microbial
449 chemosynthesis using sulphide, ammonia and methane as energy donors.

450 **4.3 Monsoon mixing in Tillari Reservoir:**

451 The reservoir gets vertically mixed during the months of July, August and September due to a
452 combination of lower atmospheric temperature, strong winds and inflow of relatively cold
453 water during the southwest monsoon. Nitrate concentrations are moderately high throughout
454 the water column, although variable from one year to another. The mean water-column nitrate
455 concentration were $7.26 \pm 2.8 \mu\text{M}$ ($n = 10$) in 2011, $9.29 \pm 0.8 \mu\text{M}$ ($n = 10$) in 2014, and
456 $8.13 \pm 4.7 \mu\text{M}$ ($n = 9$) in 2015. The isotopic composition of nitrate also showed inter-annual
457 variability. While the water column was uniformly nitrate-replete in 2014, the epilimnetic (0-
458 5 m) nitrate concentrations in 2011 and 2015 were markedly lower than those at deeper
459 depths (Fig.7), except at two deepest samples in 2015. This may indicate nitrate uptake by
460 phytoplankton. However, considering its high concentration in rainwater, ammonium is
461 expected to compete with nitrate for phytoplankton uptake. Moreover, the $\delta^{15}\text{N}$ of nitrate in
462 the epilimnion was lower in 2011 and 2015 than in 2014. In fact, elevated values of $\delta^{15}\text{N}$ -
463 NO_3^- ($>8\text{‰}$) occurred throughout the water column in 2014 when the nitrate concentration
464 was also generally higher as compared to the other two years. To investigate the cause of this
465 variability, water samples from six upstream stations along the Tillari River along with a

466 rainwater sample at the main station were collected in 2015. The nitrate concentrations
467 ranged from 1.8 μM at the most upstream station to 9.4 μM close to our main sampling site.
468 The ranges of $\delta^{15}\text{N}$ and $\delta^{18}\text{O}$ of NO_3^- at these stations were 0.4-6.8‰ and 11-27‰,
469 respectively. The rainwater sample had a nitrate content of 13.89 μM (ammonium = 24.4 μM)
470 and yielded $\delta^{15}\text{N}$ and $\delta^{18}\text{O}$ values of -2.9‰ and 88.7‰, respectively. Nitrate in wet
471 deposition is usually characterised by high $\delta^{18}\text{O}$ ($> 60\text{‰}$) (Kendall et al., 2007; Thibodeau et
472 al., 2013) and low $\delta^{15}\text{N}$ (-10 to $+5 \text{‰}$) (Heaton et al., 2004) values. Unfortunately, the
473 concentration and isotopic composition of these end members (river runoff and atmospheric
474 deposition) do not explain the data from the Tillari especially from the 2015. Based on the
475 high concentration of nitrate in rainwater, it is tempting to suggest that it could be an
476 important source, but the isotopic data show a mismatch. The $\delta^{13}\text{C}$ -POC values in the
477 epilimnion decreased to nearly -30‰ presumably due to a combination of lower primary
478 productivity and inputs of organic matter through runoff. Even though the latter was not
479 measured POC derived from land vegetation is expected to be isotopically light. The POM
480 data show the ingress of a nearly 30m thick parcel of water from the Tillari River into the
481 reservoir. This ingress is apparent below 5m depth by distinct $\delta^{13}\text{C}$ and $\delta^{15}\text{N}$ of POM. The
482 $\delta^{13}\text{C}$ -POC increases from -30.9‰ ($\pm 0.1\text{‰}$) in the upper 5m to -25.4‰ ($\pm 1\text{‰}$) between 5m
483 and 40m. Below 40m, the mean $\delta^{13}\text{C}$ -POC was -26.5‰ ($\pm 1.7\text{‰}$). The mean $\delta^{15}\text{N}$ of the
484 intermediate water parcel was $5.97 \pm 2\text{‰}$, as compared to $5.49 \pm 3\text{‰}$ in the bottom waters and
485 $3.96 \pm 2\text{‰}$ in the upper 5m. The isotopic data correspond well with the ancillary chemical
486 parameters, in that the water parcel had a distinct thermal signature (cooler by nearly 2°C). It
487 also possessed higher levels of nitrate and lower levels of DO and chlorophyll-*a*.

488 Thus, looking solely at the high nitrate concentrations in the water column, atmospheric wet
489 deposition may be a major nitrate source to the water column during the monsoon season.
490 However, this inference is based on a single measurement where the isotopic composition is

491 also different. Moreover, the river water is also rain-fed and it is not clear why its isotopic
492 composition is much lower at the most upstream station. At the same time, the isotopic
493 composition of POM indicates influence of the upstream waters. Variable inputs from the
494 atmosphere and by river runoff to the DIN pool probably account for the interannual
495 variability, but more studies are needed to identify and quantify these contributions in detail.

496 **5. Summary and Conclusions:**

497 Using stable isotopes of nitrate, ammonium and particulate organic matter, we have been able
498 to identify distinct water column conditions and transformation processes of reactive nitrogen
499 in the Tillari Reservoir. The reservoir gets vertically mixed during the southwest monsoon
500 season as well as in winter; the water column remained stratified during other parts of the
501 year. The most intense stratification occurs during summer just before the monsoon onset.
502 Relative importance of microbial processes such as nitrification, denitrification,
503 ammonification and sulphate reduction in the water column varied depending on intensity of
504 stratification and associated DO levels in the hypolimnion. These processes produced unique
505 isotopic signatures in the dissolved and particulate matter. Our results suggest the occurrence
506 of microbial chemosynthesis using methane and ammonium as primary C- and N- sources,
507 producing organic matter in the anoxic bottom waters that is highly depleted in ^{13}C and ^{15}N
508 content. The thermocline in the Tillari Reservoir has been known to harbour photoautotrophic
509 sulphur bacteria during peak stratification periods (Kurian et al., 2012). We also found strong
510 signatures of nitrification within this zone during summer stratification. Autochthonous
511 production was the principal source of organic matter in the epilimnion which was well-
512 oxygenated at all times, although productivity was significantly lower during the monsoon
513 period due to light-limited conditions. Nitrate was the preferred DIN source in the
514 epilimnion. When nitrate loss occurred in the hypolimnion, the preferred DIN species

515 switched from nitrate to ammonium. Isotopic measurement of precipitation and upstream
516 river samples during one seasonal sampling provided some insight into sources of nitrogen,
517 but the observed inter-annual variability could not be explained. Overall, solar intensity,
518 water depth and redox conditions appear to be the major factors controlling biogeochemical
519 cycling in this pristine reservoir.

520 **Acknowledgements:**

521 We thank the Director, CSIR-NIO for providing necessary support for this work and the
522 management body of the Tillari reservoir for permission to carry out this study. This research
523 was carried out as a part of INDIAS IDEA project funded by the Council of Scientific &
524 Industrial Research (CSIR). The authors wish to thank Mark Altabet and Laura Bristow for
525 sharing their expertise. We thank Prof. Sugata Hazra and the School of Oceanographic
526 Studies, Jadavpur University for their support and encouragement. Puja Satardekar is
527 acknowledged for analyzing the nutrient samples. Sujal Bhandodkar (DTP section, CSIR-NIO)
528 is thanked for her creative inputs. P. Bardhan thanks CSIR for the award of Senior Research
529 Fellowship. The authors are also grateful to Ms. Maya MV for her initial assistance in
530 isotopic analyses and to Mr. H. Dalvi, Mr. A. Methar, Mr. Jonathan and Mr. Sumant for their
531 help during field work. This is NIO Contribution no. XXXX.

532 **References**

533 Altabet, M. A.: Variations in nitrogen isotopic composition between sinking and suspended
534 particles: Implications for nitrogen cycling and particle transformation in the open ocean,
535 *Deep-Sea Res.*, 35, 535–554, 1988.

536

537 Altabet, M. A.: Isotopic tracers of the marine nitrogen cycle, in: *Marine organic matter:
538 Chemical and biological markers*, edited by: Volkman, J., *The handbook of environmental
539 chemistry*, Springer-Verlag, 251–293, 2006.

540

541 Bastviken, D., Cole, J. J., Pace, M., and Tranvik, L.: Methane emissions from lakes:
542 Dependence of lake characteristics, two regional assessments, and a global estimate, *Glob.
543 Biogeochem. Cy.*, 18:GB4009, doi: 10.1029/2004GB002238, 2004.

544

545 Böttcher, J., Strebel, O., Voerkelius, S., and Schmidt, H.-L.: Using isotope fractionation of
546 nitrate-nitrogen and nitrate-oxygen for evaluation of microbial denitrification in a sandy
547 aquifer, *J. Hydrol.*, 114, 413–424, doi: 10.1016/0022-1694(90)90068-9, 1990.
548

549 Brandes, J. A., Devol, A. H., Yoshinari, T., Jayakumar, D. A., and Naqvi, S. W. A.: Isotopic
550 composition of nitrate in the central Arabian Sea and eastern tropical North Pacific: A tracer
551 for mixing and nitrogen cycles, *Limnol. Oceanogr.*, 43, 1680–1689, doi:
552 10.4319/lo.1998.43.7.1680, 1998.
553

554 Bratkic, A., Sturm, M., Faganeli, J., and Ogrinc, N.: Semi-annual carbon and nitrogen isotope
555 variations in the water column of Lake Bled, NW Slovenia, *Biogeosciences*, 9, 1–11. doi:
556 10.5194/bg-9-1-2012, 2012.
557

558 Burns, D. A. and Kendall, C.: Analysis of ¹⁵N and ¹⁸O sources in runoff at two watersheds in
559 the Catskill Mountains of New York, *Water Resour. Res.*, 38, 1051, doi: 10.1029/
560 2001WR000292, 2002.
561

562 Carpenter, E. J., Harvey, H. R., Fry, B., and Capone, D. G.: Biogeochemical tracers of the
563 marine cyanobacterium *Trichodesmium*, *Deep-Sea Res. Pt. I*, 44, 27–38, 1997.
564

565 Casciotti, K. L., Sigman, D. M., Galanter Hastings, M., Bohlke, J. K., and Hilkert, A.:
566 Measurement of the oxygen isotopic composition of nitrate in seawater and freshwater using
567 the denitrifier method, *Anal. Chem.*, 74, 4905–4912, 2002.
568

569 Casciotti, K. L., Sigman, D. M., and Ward, B. B.: Linking diversity and stable isotope
569 fractionation in ammonia-oxidizing bacteria, *Geomicrobiol. J.*, 20, 335–353, 2003.
570

571 Chen, F. J. and Jia, G. D.: Spatial and seasonal variations in $\delta^{13}\text{C}$ and $\delta^{15}\text{N}$ of particulate
572 organic matter in a dam-controlled subtropical river, *River Res. Appl.*, 25, 1169–1176, doi:
573 10.1002/rra.1225, 2009.
574

575 Chen, F., Jia, G., and Chen, J.: Nitrate sources and watershed denitrification inferred from
576 dual isotopes in the Beijiang River, South China, *Biogeochemistry*, 94, 163–174, doi:
577 10.1007/s10533-009-9316-x, 2009.
578

579 Chen, Z.X., Yu, L., Liu, W.G., Lam, M.H.W., Liu, G.J., and Yin, X. B.: Nitrogen and oxygen
580 isotopic compositions of water-soluble nitrate in Taihu Lake water system, China: implication
581 for nitrate sources and biogeochemical process, *Environ Earth Sci.*, 1, 217–223, 2014.
582

583 Christofi, N., Preston, T. and Stewart, W.D.P.: Endogenous nitrate production in an
584 experimental enclosure during summer stratification, *Water research*, 15(3), 343-349, doi:
585 10.1016/0043-1354(81)90039-7, 1981.
586

587 Cifuentes, L. A., Sharp, J. H., and Fogel, M. L.: Stable carbon and nitrogen isotope
588 biogeochemistry in the Delaware Estuary, *Limnol. Oceanogr.*, 33, 1102–1115, 1988.
589

590 Cline, J.D.: Spectrophotometric determination of hydrogen sulfide in natural waters, *Limnol.*
591 *Oceanogr.*, 14, 454–458, 1969.
592

593 Dähnke, K., and Thamdrup, B.: Nitrogen isotope dynamics and fractionation during
594 sedimentary denitrification in Boknis Eck, Baltic Sea, *Biogeosciences*, 10, 3079–3088. doi:
595 10.5194/bg-10-3079-2013, 2013.
596
597 Delwiche, C. C., and Stein, P. L.: Nitrogen isotope fractionation in soil and microbial
598 reactions, *Environ. Sci. Tech.*, 4, 929-935, 1970.
599
600 Feigin, A., Shearer, G., Kohl, D.H. and Compton, B.: The amount and nitrogen -15 content
601 of nitrate in soil profiles from two central Illinois fields in a corn-soybean rotation, *Soil Sci.*
602 *Soc. Amer. Proc.*, 38, 465–471, 1974.
603
604 Finlay, J. C., Sterner, R. W., and Kumar, S.: Isotopic evidence for in-lake production of
605 accumulating nitrate in Lake Superior, *Ecol. Appl.*, 17, 2323–2332, doi: 10.1890/07-0245.1,
606 2007.
607
608 Granger, J., Sigman, D. M., Lehmann, M. F., and Tortell, P. D.: Nitrogen and oxygen isotope
609 fractionation during dissimilatory nitrate reduction by denitrifying bacteria, *Limnol.*
610 *Oceanogr.*, 53, 2533–2545, 2008.
611
612 Grasshoff, K., Ehrhardt, M., and Kremling, K.: *Methods of seawater analysis*, 2 Edn., 419
613 pp., Weinheim: Verlag Chemie., 1983.
614 Gu, B., Chapman, A. D., and Schelske, C. L.: Factors controlling seasonal variations in stable
615 isotope composition of particulate organic matter in a soft water eutrophic lake, *Limnol.*
616 *Oceanogr.*, 51, 2837-2848, 2006.
617
618 Hadas, O., Altabet, M. A., and Agnihitori, R.: Seasonally varying nitrogen isotope
619 biogeochemistry of particulate organic matter in lake Kinneret, Israel, *Limnol. Oceanogr.*, 54,
620 75–85, 2009.
621
622 Heaton, T. H. E.: Isotopic studies of nitrogen pollution in the hydrosphere and atmosphere: A
623 review, *Chem. Geol.*, 59, 87-102, 1986.
624
625 Hoch, M. P., Fogel, M. L., and Kirchman, D. L.: Isotope fractionation associated with
626 ammonium uptake by a marine bacterium, *Limnol. Oceanogr.*, 37, 1447-1459, 1992.
627
628 Holmes, R. M., McClelland, J. W., Sigman, D. M., Fry, B., and Peterson, B. J.: Measuring
629 $^{15}\text{N-NH}_4^+$ in marine, estuarine and fresh waters: an adaptation of the ammonia diffusion
630 method for samples with low ammonium concentrations, *Mar. Chem.*, 60, 235–243,
631 doi: 10.1016/S0304-4203(97)00099-6, 1998.
632
633 Hu, H., Bourbonnais, A., Larkum, J., Bange, H. W., and Altabet, M. A.: Nitrogen cycling in
634 shallow low oxygen coastal waters off Peru from nitrite and nitrate nitrogen and oxygen
635 isotopes. *Biogeosciences Discussions* 12, 7257-7299, doi: 10.5194/bgd-12-7257-2015, 2015.
636
637 Junet, A. de, Abril, G., Gu'erin, F., Billy, I., and Wit, R. de.: A multi-tracers analysis of
638 sources and transfers of particulate organic matter in a tropical reservoir (Petit Saut, French
639 Guiana), *River Res. Appl.*, 25, 253–271, doi:10.1002/rra.1152, 2009.

640 Kendall, C.: Tracing nitrogen sources and cycling in catchments, in: Isotope tracers in
641 catchment hydrology, edited by: Kendall, C. and McDonnell, J.J., Elsevier, Amsterdam, The
642 Netherlands, 519-576, 1998.

643

644 Kendall, C., Silva, S. R., and Kelly, V. J.: Carbon and nitrogen isotopic compositions of
645 particulate organic matter in four large river systems across the United States, *Hydrol.*
646 *Process.*, 15, 1301-1346, doi: 10.1002/hyp.216, 2001

647 Kendall, C., Elliott, E. M., and Wankel, S. D.: Tracing anthropogenic inputs of nitrogen to
648 ecosystems, Chapter 12, in: *Stable Isotopes in Ecology and Environmental Science*, edited
649 by: Michener, R. H. and Lajtha, K., 2nd Edition, Blackwell Publishing, 375-449, 2007.

650

651 Kritee, K., Sigman, D.M., Granger, J., Ward, B.B., Jayakumar, A., and Deutsch, C.: Reduced
652 isotope fractionation by denitrification under conditions relevant to the ocean, *Geochim.*
653 *Cosmochim. Acta*, 92, 243-259, doi:10.1016/j.gca.2012.05.020, 2012.

654

655 Kurian, S., Roy, R., Repeta, D.J., Gauns, M., Shenoy, D.M., Suresh, T., Sarkar, A.,
656 Narvenkar, G., Johnson, C.G., and Naqvi, S.W.A.: Seasonal occurrence of anoxygenic
657 photosynthesis in Tillari and Selaulim reservoirs, Western India, *Biogeosciences*, 9, 2485-
658 2495, doi:10.5194/bg-9-2485-2012, 2012.

659

660 Lehmann, M. F., Reichert, P., Bernasconi, S. M., Barbieri, A., and McKenzie, J.: Modelling
661 nitrogen and oxygen isotope fractionation during denitrification in a lacustrine redox-
662 transition zone, *Geochim. Cosmochim. Ac.*, 67, 2529-2542, doi: 10.1016/S0016-
663 7037(03)00085-1, 2003

664

665 Lehmann, M. F., Bernasconi, S., McKenzie, J., Barbieri, A., Simona, M., and Veronesi, M.:
666 Seasonal variation of the $\delta^{13}\text{C}$ and $\delta^{15}\text{N}$ of particulate and dissolved carbon and nitrogen in
667 Lake Lugano: Constraints on biogeochemical cycling in a eutrophic lake, *Limnol. Oceanogr.*,
668 49, 415-429, 2004.

669

670 Maya, M. V., Karapurkar, S. G., Naik, H., Roy, R., Shenoy, D. M., and Naqvi, S. W. A.: Intra-
671 annual variability of carbon and nitrogen stable isotopes in suspended organic matter in
672 waters of the western continental shelf of India, *Biogeosciences*, 8, 3441- 3456,
673 doi:10.5194/bg-8-3441-2011, 2011.

674

675 McIlvin, M. R. and Altabet, M. A.: Chemical conversion of nitrate and nitrite to nitrous oxide
676 for nitrogen and oxygen isotopic analysis in freshwater and seawater, *Anal. Chem.*, 77, 5589-
677 5595, doi: 10.1021/ac050528s, 2005.

678

679 Mengis, M., Schiff, S. L., Harris, M., English, M. C., Aravena, R., Elgood, R. J., and
680 MacLean, A.: Multiple geochemical and isotopic approaches for assessing ground water NO_3^-
681 elimination in a riparian zone, *Ground Water*, 37, 448-457, 1999.

682

683 Narvenkar, G., Naqvi, S. W. A., Kurian, S., Shenoy, D. M., Pratihary, A. K., Naik, H., Patil,
684 S., Sarkar, A., and Gauns, M.: Dissolved methane in Indian freshwater reservoirs, *Environ*
685 *Monit Assess.*, 185(8), 6989-6999, 2013.

686

687 Olleros, T.: Kinetische Isotopeneffekte der Arginase- und Nitratreduktase-Reaktion: Ein
688 Beitrag zur Aufklärung der entsprechenden Reaktionsmechanismen, Ph.D. dissertation,
689 Technische Universität München-Weihenstephan, Germany, 1983.

690
691 Pang, P. C., and Nriagu, J. O.: Isotopic variations of the nitrogen in Lake Superior, *Geochim.*
692 *Cosmochim. Acta*, 41, 811–814, doi: 10.1016/0016-7037(77)90051-5, 1977.
693
694 Prokopenko, A. A., and Williams, D.F.: Depleted methane-derived carbon in waters of Lake
695 Baikal, Siberia, *Hydrobiol.*, 544, 279-288, 2005.
696
697 Savoye, N., David, V., Morisseau, F., Etcheber, H., Abril, G., Billy, I., Charlier, K., Oggian,
698 G., Derriennic, H., and Sautour, B.: Origin and composition of particulate organic matter in a
699 macrotidal turbid estuary: the Gironde Estuary, France, *Estuar. Coast. Shelf Sci.*, 108, 16-28,
700 doi: 10.1016/j.ecss.2011.12.005, 2012.

701 Seitzinger, S. P.: Denitrification in freshwater and coastal marine ecosystems: Ecological and
702 Geochemical significance, *Limnol. Oceanogr.*, 33, 702–724, 1988.
703
704 Sigman, D. M., Robinson, R., Knapp, A. N., Van Geen, A., McCorkle, D. C., Brandes, J. A.,
705 and Thunell, R. C.: Distinguishing between water column and sedimentary denitrification in
706 the Santa Barbara Basin using the stable isotopes of nitrate. *Geochem. Geophys. Geosy.*, 4,
707 1040, doi:10.1029/2002GC000384, 2003.
708
709 Sigman, D. M., Granger, J., DiFiore, P. J., Lehmann, M. M., Ho, R., Cane, G., and van Geen,
710 A.: Coupled nitrogen and oxygen isotope measurements of nitrate along the eastern North
711 Pacific margin, *Global Biogeochem. Cy.*, 19, GB4022, doi:10.1029/2005GB002458, 2005.
712
713 Subramanya, K.: *Engineering Hydrology*, 4th edition, McGraw-Hill Publishing, New Delhi,
714 2013.
715
716 Sukumar, R., Suresh, H. S., and Ramesh, R.: Climate change and its impact on tropical
717 montane ecosystems in southern India. *J. Biogeogr.*, 22, 533-536, 1995.
718
719 Thibodeau, B., Hélie, J.-F., and Lehmann, M. F.: Variations of the nitrate isotopic
720 composition in the St. Lawrence River caused by seasonal changes in atmospheric nitrogen
721 inputs, *Biogeochemistry*, 115, 287–298, 2013.
722
723 Thunell, R. C., Sigman, D. M., Muller-Karger, F., Astor, Y., and Varela, R.: Nitrogen isotope
724 dynamics of the Cariaco Basin, Venezuela, *Global Biogeochem. Cy.*, 18, GB3001,
725 doi:10.1029/2003GB002185, 2004.
726
727 Voss, M., Dippner, J. W., and Montoya, J. P.: Nitrogen isotope patterns in the oxygen-
728 deficient waters of the Eastern Tropical North Pacific Ocean, *Deep-Sea Res. Pt. 1*, 48, 1905–
729 1921, doi:10.1016/S0967-0637(00)00110-2, 2001.
730
731 Wada, E. and Hattori, A.: Nitrogen isotope effects in the assimilation of inorganic compounds
732 by marine diatoms, *Geomicrobiol. J.*, 1, 85–101, 1978.
733
734 Wada, E.: Nitrogen isotope fractionation and its significance in biogeochemical processes
735 occurring in marine environments, in: *Isotope Marine Chemistry*, edited by: Goldberg, E. D.,
736 Horibe, Y., and Saruhashi, K., Uchida Rokakuho Pub. Co., Tokyo, 375–398, 1980.
737

738 Wankel, S. D., Kendall, C., Pennington, J. T., Chavez, F. P., and Paytan, A.: Nitrification in
739 the euphotic zone as evidenced by nitrate dual isotopic composition: Observations from
740 Monterey Bay, California, *Global Biogeochem. Cy.*, 21, GB2009,
741 doi:10.1029/2006gb002723, 2007.
742
743 Wenk, C. B., Zopfi, J., Bles, J., Veronesi, M., Niemann, H., and Lehmann, M. F.:
744 Community N and O isotope fractionation by sulfide-dependent denitrification and anammox
745 in a stratified lacustrine water column, *Geochim. Cosmochim. Acta*, 125, 551-563, 2014.

746 Whiticar, M. J., Faber, E., and Schoell, M.: Biogenic methane formation in marine and
747 freshwater environments:CO₂ reduction vs. acetate fermentation-isotope evidence, *Geochim*
748 *Cosmochim Acta*, 50, 693-709, 1986.
749
750
751
752
753
754
755
756
757
758
759

760

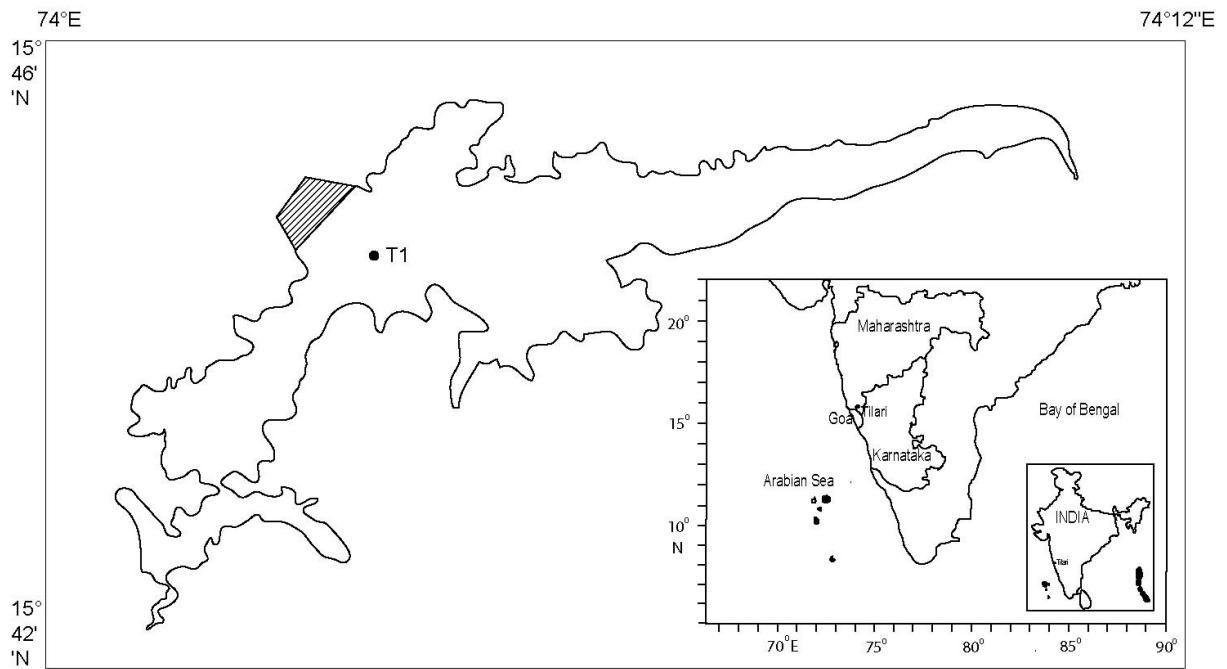
761 Table 1: The values of nitrogen (ϵ^{15}) and oxygen (ϵ^{18}) isotope effects for denitrification as
 762 reported from some natural systems as well as laboratory cultures.

763
 764

Study Area	ϵ^{15} (‰)	ϵ^{18} (‰)	Reference
Cariaco Basin, Venezuela			
Beijiang River, China		8.5	
Boknis Eck, Baltic Sea		15.8	
Lake Lugano, Switzerland		6.6	
Groundwater		18.3	
Denitrifier culture		15	
Denitrifier culture			
Open-ocean OMZs			
Shallow groundwater aquifer		8	
Tillari reservoir, India	8.73	10.74	This study

765
 766
 767
 768
 769
 770
 771
 772
 773
 774
 775
 776
 777
 778
 779
 780
 781
 782
 783
 784

785 **Figure 1: Map of the sampling location (Tillari Reservoir). T1 shows the main sampling**
786 **location at the deepest point of the reservoir.**



787

788

789

790

791

792

793

794

795

796

797

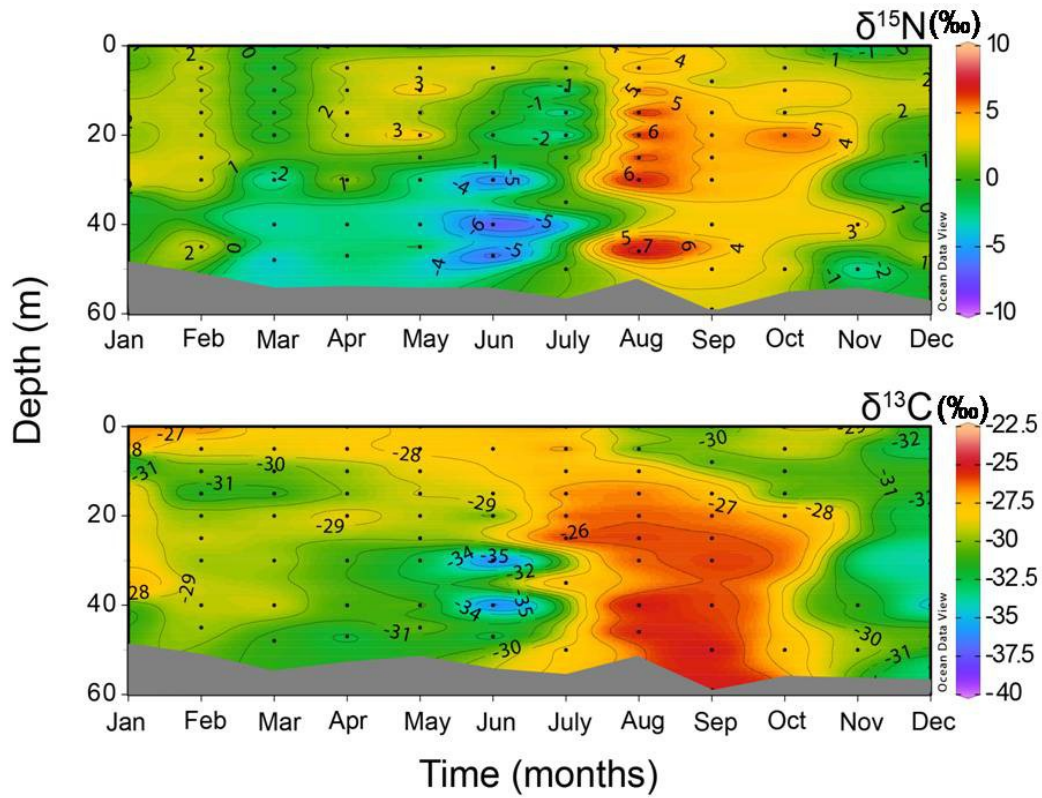
798

799

800

801

802 **Figure 2: Mean annual variations of $\delta^{15}\text{N-POM}$ and $\delta^{13}\text{C-POM}$ at the main sampling**
803 **location.**



804

805

806

807

808

809

810

811

812

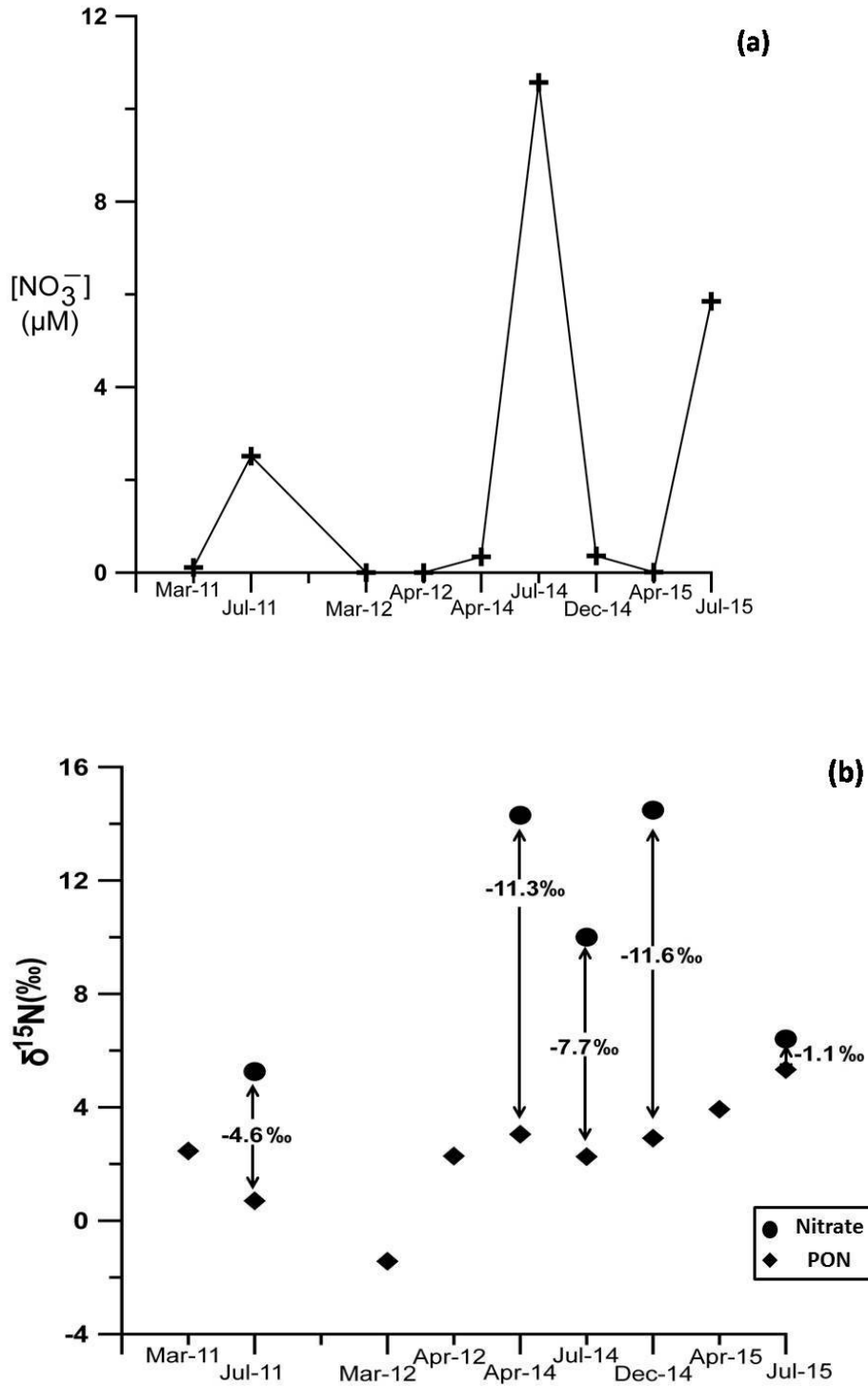
813

814

815

816

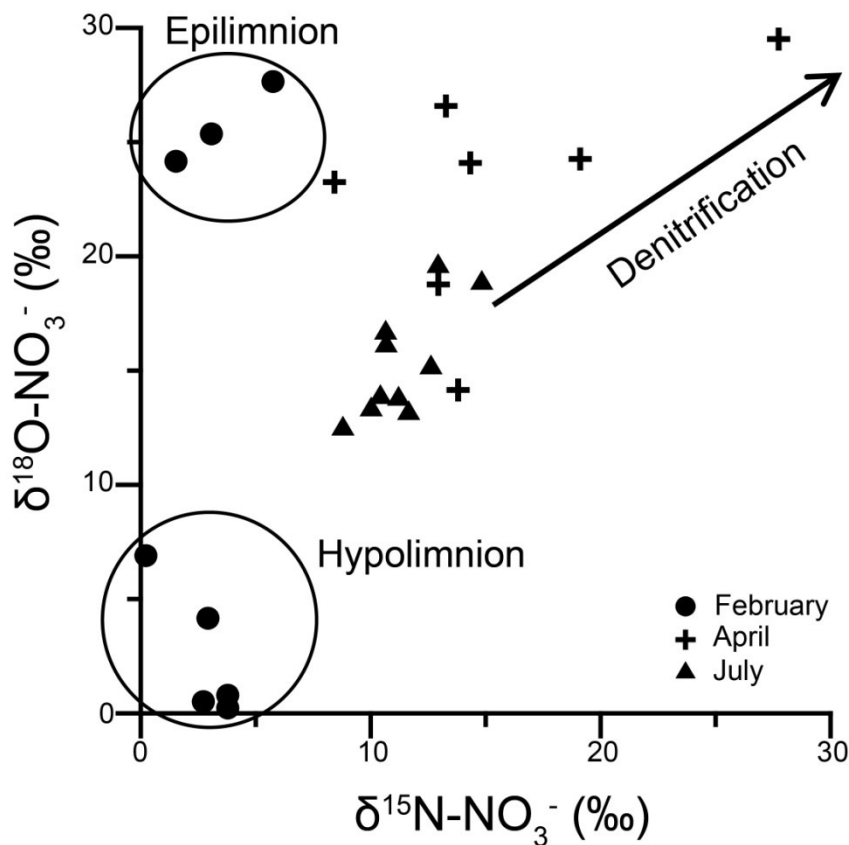
817 **Figure 3: Time-series of nitrate concentrations (a) and $\delta^{15}\text{N}$ of dissolved nitrate and**
 818 **POM in the epilimnion (0-5 m) (b). The isotopic differences between the dissolved and**
 819 **particulate species have been denoted by arrows. Each data point represents one**
 820 **sample. Each data point represents a single sample.**



821

822

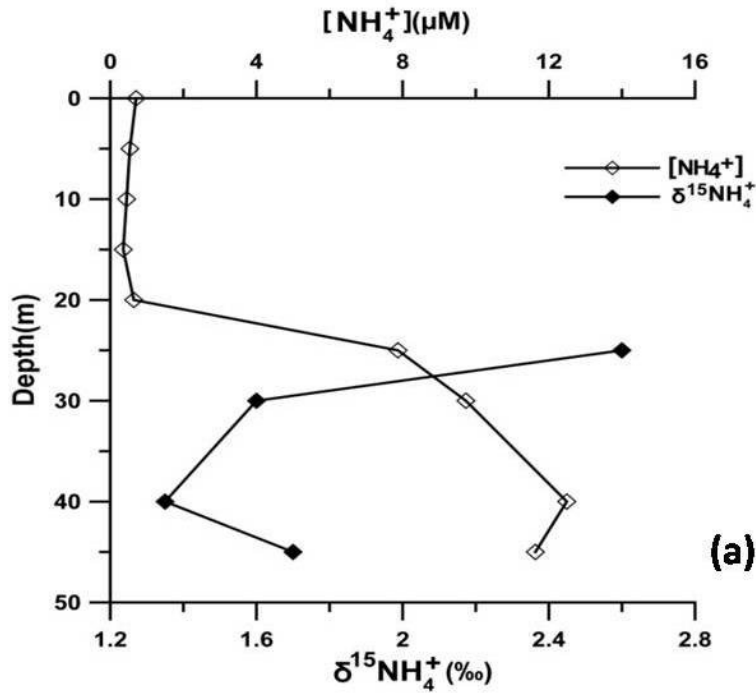
823 **Figure 4: Nitrogen and oxygen isotopic composition of dissolved nitrate during three**
824 **different periods in 2014. February represents the early or weak stratification period**
825 **with two distinct clusters of epilimnetic (0-10 m) and hypolimnetic (15-48 m) samples.**
826 **April is a period of intense water-column stratification and denitrification signal is**
827 **observed in the bottom waters. July is a period of monsoon holomixis when the water**
828 **column has uniformly high nitrate values.**



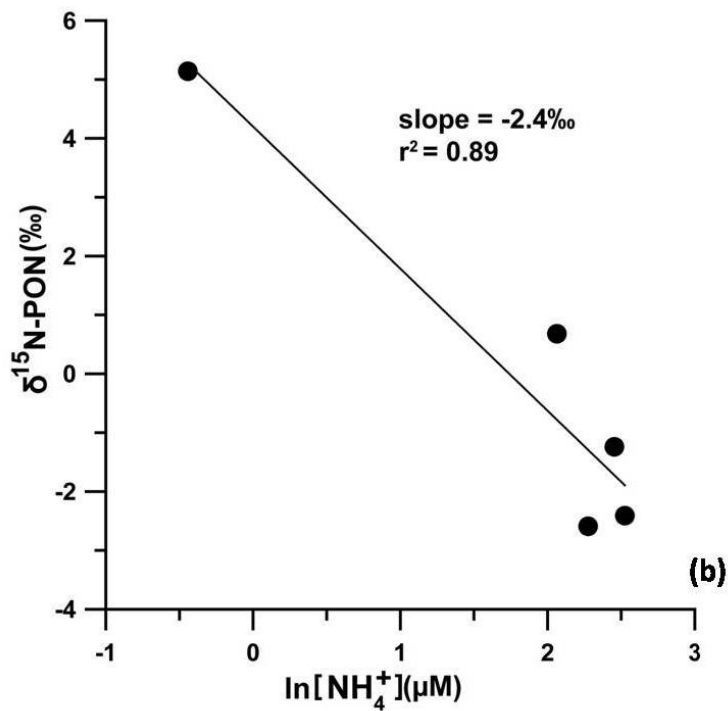
829
830
831
832
833
834
835

836 Figure 5: (a) Depth-wise variations of ammonium concentration and $\delta^{15}\text{N-NH}_4^+$ in May
 837 2012. (b) Plot of $\delta^{15}\text{N-PON}$ versus $\ln(\text{NH}_4^+)$. The negative linear correlation yields a
 838 fractionation factor (ϵ) of -2.4‰. Each data point represents a single sample.

839

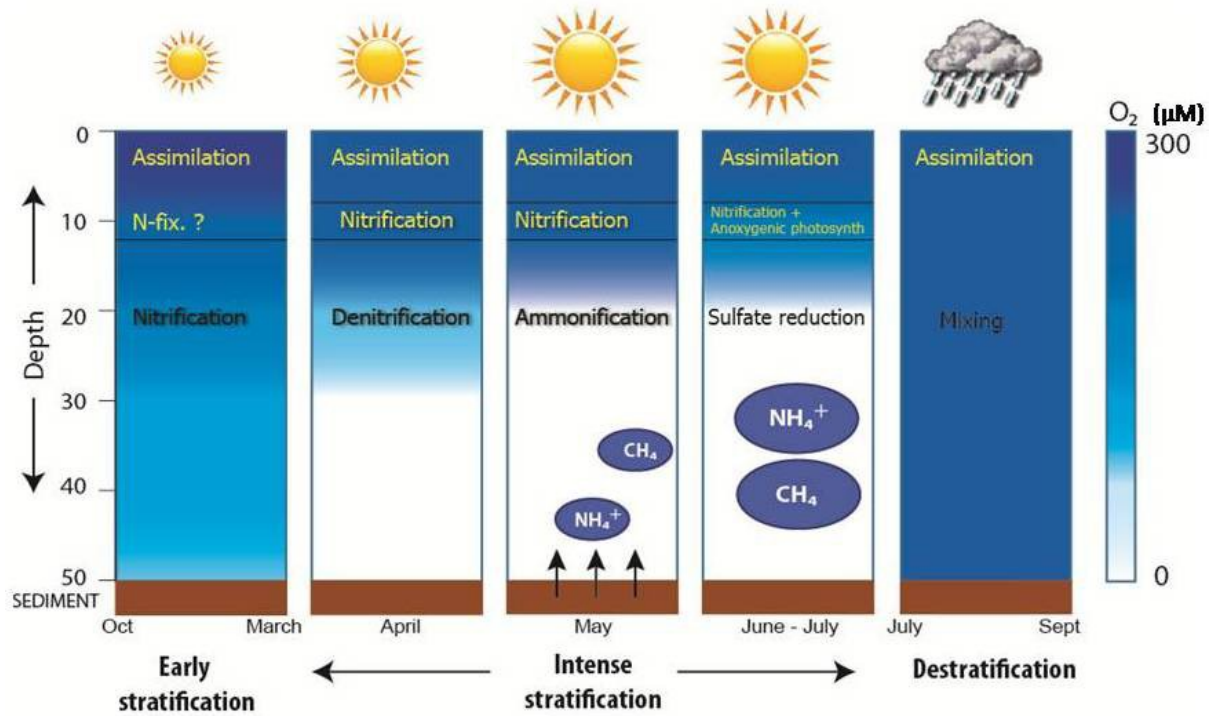


840



841

842 **Figure 6: Schematic diagram depicting major biogeochemical processes taking place in**
 843 **the Tillari Reservoir over an annual cycle. This information is based on monthly**
 844 **sampling in the reservoir for several years (Shenoy et al., manuscript in preparation)**



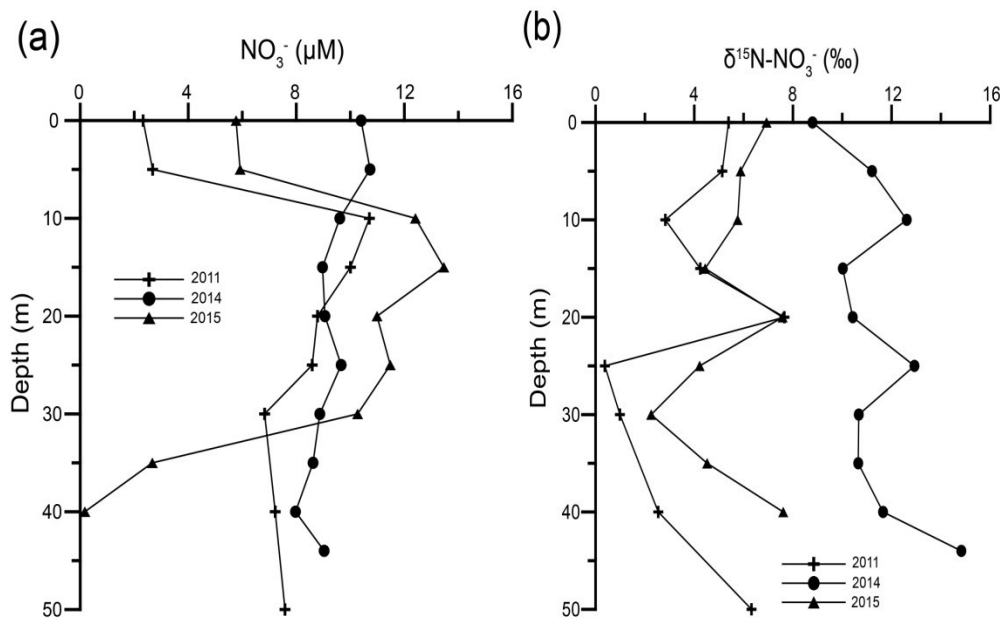
845
 846
 847
 848
 849
 850
 851
 852
 853
 854
 855
 856

857 **Figure 7: Vertical profiles of NO_3^- (a) and $\delta^{15}\text{N}\text{-NO}_3^-$ (b) during monsoon mixing in 2011,**
858 **2014 and 2015. Each profile is from one field trip during the peak SWM in a given year**
859 **with each data point representing one sample.**

860

861

862



863